

Effect of using a Dynamic Absorber On Vibrations of an Opposed-Piston Ultralight Aircraft Engine

Mohammad Reza Najafi

Department of Mechanical Engineering,
University of Imam Hossein comprehensive, Iran
E-mail: drmrnajafi@ihu.ac.ir

Saeed Mahjoub Moghadas *

Department of Mechanical Engineering,
University of Imam Hossein comprehensive, Iran
E-mail: smahjoubmoghadas@ihu.ac.ir

*Corresponding author

Mojtaba Moradi

Department of Mechanical Engineering,
University of Imam Hossein comprehensive, Iran
E-mail: alabd.rasool@chmail.ir

Received: 18 August 2020, Revised: 1 December 2020, Accepted: 13 December 2020

Abstract: In this paper, vibrations reduction of piston engine of ultralight aircrafts was studied with considering a combination of experimental, analytical and numerical methods. Analytical equations of dynamic absorber were obtained. Afterward, experimental test was used to determine the system torque. Due to the difficulty of obtaining experimental data, the amount of angular acceleration and then velocity and angular displacement were calculated numerically using MATLAB software and verified with experimental results with a difference of less than 2%. Different components of the system were designed with reverse engineering method using SolidWorks software. After data transmission to Adams software, vibrational analysis of the system was performed and validated with analytical results with a difference of less than 1.91%. A suitable dynamic absorber was selected. The results showed that engine vibrations is reduced up to 40%.

Keywords: Angular Velocity, Dynamic Absorber, Piston Engine, Ultralight Aircraft, Vibration

Reference: Mohammad Reza Najafi, Saeed Mahjoub Moghadas, and Mojtaba Moradi, "Effect of using a Dynamic Absorber On Vibrations of an Opposed-Piston Ultralight Aircraft Engine", Int J of Advanced Design and Manufacturing Technology, Vol. 14/No. 1, 2021, pp. 91–99.
DOI: 10.30495/admt.2021.1907260.1212

Biographical notes: **Mohammad Reza Najafi** is a PhD student in Mechanical Engineering at the University of Imam Hossein comprehensive, Iran. His current research interests include vibration and dynamic. **Saeed Mahjoub Moghadas** is Associate Professor of Mechanical engineering at the University of Imam Hossein comprehensive since 1986, Iran. He received doctorate with the thesis subjected for "Internal Combustion Engines Control and Diagnostics through Instantaneous Speed of Rotation Analysis" at L'ensam university in Paris, France, 1985. He has authored 20 books and translated 15 others in the field of dynamic, vibration and control. **Mojtaba Moradi** is received his MSc in Mechanical Engineering from Imam Hossein comprehensive University.

1 INTRODUCTION

Today, it is one of importance for industries to have dynamic solutions for disturbing vibrations in the case of dynamic systems and characterizing their dynamic behavior. In this field, designers and engineers have concentrated on vibrations reduction of aircraft engines especially in the case of ultralight aircraft due to wide application in aero-industries. Ultralight aircraft usually are equipped with piston engines to propel the aircraft structure. These aircraft engines are similar to automobiles engines structurally but they are larger and work in higher rotating velocities conditions. When the natural frequency of engine reaches the external excitation frequency, the resonance phenomenon occurs which leads to maximum displacement of vibrating system that it can cause to its devastation.

It is really important to concern with the engine vibrations as well as dynamic behavior due to structural deteriorative events as in case of resonance effect [1]. The internal torque variation of the piston engine generates resonance for crankshaft and propeller [2]. One of the easiest solutions for inhibition of deteriorative vibrations is a dynamic absorber that is recommended to use in each step of design, fabrication till running. The main terms of dynamic absorbers are such as mass, hardness, and structural damping which determine the natural frequency of structure [3–5]. The engine vibrations may originate from a lack of damping of reciprocating arrays, lack of isolator, and dynamic absorbers [6-7].

Genta & et al. [8-9] studied the stability of rotating blade arrays and the effect of disk-blade interaction on the disc. If the blade length exceeds from the disc radius, the resonance occurs in a range more than critical velocity, in-plane motions of the blade make instability and blades are stable in the case of smaller disc length. The instability is not affected by blade damping even if internal damping occurs. Lin & et al. analyzed the free vibration of a non-uniform beam with restrained root and with a concentrated mass at the end [10]. Dynamic analysis of concentrated mass effect, devastating effect of vibration, and Green function for beam are investigated. Rao & et al. represented a method for approximate calculation of the natural frequencies as well as the number of modes for a finite element in continuum systems [11].

Turhan and Bulut have investigated the effect of multistage rotor-blade systems vibrations and natural frequency due to rotor torsional vibration modes [12]. Yang and Huang have investigated the modal analysis of shaft-disk-blades systems vibrations using the Galerkin method [13]. The resonance occurs when an excitation frequency equal to the number of free vibrations of crankshaft occurs. The gas pressure torque leads to periodic forces with a frequency quantity twice the

fundamental vibrations frequency [14]. The opposed piston engines are widely used and studied in many industrial cases [15–19]. It is difficult to always analyze the motor engine of aircraft experimentally, so the numerical analysis is needed to select suitable vibration absorbers. The type and qualification of absorbers are investigated in many types of research [20–27].

The aim of this work is reduction of vibrations of ultralight aircraft engine. Hence, application of these type of aircraft is noticeably increasing but any access to experimental test of vibrations increases costs and demands equipment. Thus theoretical and numerical analysis of these engines become more important which is considered in our work. The analysis of the dynamic absorber is carried out and the related equations are calculated. Afterward, experimental measurement is carried out to obtain torque of piston engine during different rotating velocity. Due to experimental limitations of measurements, analytical analysis is employed. Therefore, theoretical calculations are written in MATLAB code and validated with experimental results. Various components are designed with reverse engineering method using SolidWorks software to analyze system vibration. Then natural frequencies of system are calculated by transmitting data to Adams software. Finally, vibrations reduction of engine was obtained with implementing the dynamic absorber.

2 DYNAMIC ABSORBER EQUATIONS

Dynamic absorber decreases vibration amplitude so that the effect of disturbing vibrations on the piston engine decreases. The three main characteristics are mass, stiffness and damping. To reduce the amplitude of vibrations, analyses of system must be determined. Figure 1 represents the free diagram of dynamic absorber. The related equations are described as below.

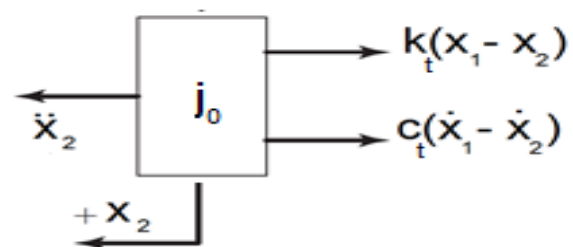


Fig. 1 Free diagram of the dynamic absorber.

$$m\ddot{x}_2 + c\dot{x}_2 + kx_2 = F\sin \omega t \quad (1)$$

Considering harmonic motion of the engine:

$$x_1(t) = X_1 \sin \omega t \quad (2)$$

$$F = X_1 \sqrt{1 + \frac{c\omega}{k}} \quad (3)$$

“Eqs. (2)-(3)” are used in order to solve “Eq. (1)”, so there is:

$$X_2 = \frac{F}{\sqrt{(k - m\omega^2)^2 + \omega^2 c^2}} \quad (4)$$

The engine vibrations are considered as a harmonic transmitted force in “Eq. (5)”.

$$\frac{\theta_2}{\theta_1} = \sqrt{\frac{k_t^2 + \omega^2 c_t^2}{(k_t - J_0 \omega^2)^2 + \omega^2 c_t^2}} \quad (5)$$

The torsional vibration amplitude (θ) ratio of the piston engine in the case of using dynamic absorber has been calculated concerning [11]. Harmonic response of a damping system is attributed to “Eq. (6)” considering “Eq. (5)”.

$$\frac{\theta}{\theta_{st}} = \frac{1}{\sqrt{(1 - r^2)^2 + (1 - 2\delta r)^2}} \quad (6)$$

The damping coefficient of vibration absorber is free of mass and hardness as in “Eq. (11)” with reference to [11]

$$\theta_{st} = \frac{M}{k_t} \quad (7)$$

$$r = \frac{\omega}{\omega_n} \quad (8)$$

$$\delta = \frac{c}{2J_0\omega_n} \quad (9)$$

$$\omega_n = \sqrt{\frac{k_t}{J_0}} \quad (10)$$

Considering “Eq. (7) to (10)”, the damping coefficient of vibration absorber is free of mass and hardness as in “Eq. (11)”. So there is:

$$c_t = \sqrt{\left(\frac{M}{\theta\omega}\right)^2 + 2k_t I_0 - \left(\frac{k_t}{\omega}\right)^2 - (\omega I_0)^2} \quad (11)$$

Because of the difficulty of torsional stiffness calculation (K_t), the term is calculated with obtaining

natural frequency (ω_n) and inertia torque I_0 . To decrease the amplitudes of the torsional vibration, the damping coefficient should be considered more than the resulted value from “Eq. (11)”. The coefficient is determined with a calculation of the amplitude of the angular vibrations and the total torque acting on the engine.

3 EXPERIMENTAL MESEARMENT

Experimental measurement is carried out to obtain amount of total torque. The rotating velocity of propeller and engine is measured using a digital camera which can analyse a movie of the rotating propeller. Fig. 2a represents the piston engine configuration. The ultralight aircraft model fabricated for experimental testing represented in “Fig. 2b”. Some properties of the engine are shown in “Table 1”.

Table 1 Qualification of 100 HP four-stroke opposed-piston engine

Parameter	Value	Parameter	Weight (Kg)
Longitudinal motion in the cylinder	61 mm	Engine and gearbox	56.6
Piston diameter	84 mm	Piston weight	0.32
Connecting rod longitudinal motion	93.75 mm	Connecting rod weight	0.474
Crank radius	30.5 mm	Crankshaft	3.58

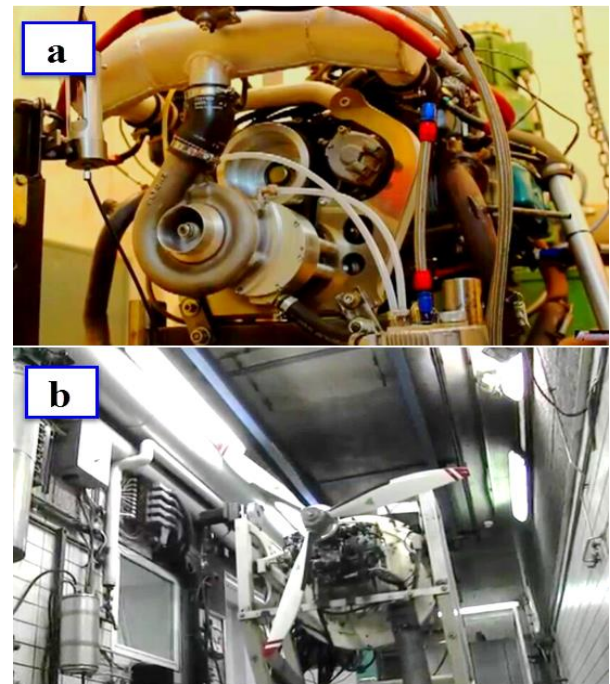


Fig. 2 (a): Piston engine configuration and (b) fabricated model of aircraft system for experimental test.

Figure 3 describes the results of engine experiments such as gas pressure on the piston, total torque in the rotating velocity range of 1849 to 5800 RPM to confirm the accuracy of the results. It represents an approximately uniform increase of torque versus increasing rotating. The maximum gas pressure value has been obtained 54 atm.

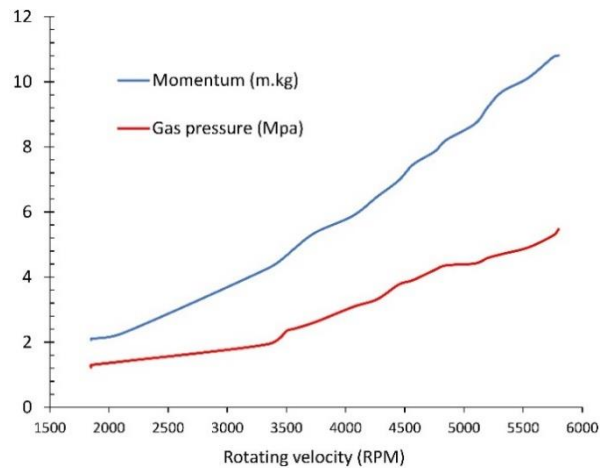


Fig. 3 Experimental results of variations of torque and gas pressure versus rotation velocity.

4 DYNAMIC ANALYSIS OF SYSTEM

Due to the limitations of the experimental method, the analytical method is used to determine the angular values of acceleration, velocity and displacement. The dynamic equations is extracted with reference to [28]. The total torque is consistent with five important terms based on “Eq. (12)” such as gas pressure torque (M_g), inertia torque of elements (M_i), the torque due to applied loads (M_l), gravity torque (M_G), and friction torque (M_f) due to contact of different parts with the axis of rotation.

$$\sum M_{total} = M_g + M_i - M_f - M_l - M_G \quad (12)$$

Analytical analysis of both terms of M_g and M_i has been studied during working time steps for a piston and the results has been generalized to four pistons [28]. To calculate the value of the gas pressure torque, instantaneous equations of torque for each piston is investigated separately in 200 steps process using MALAB software. Gas pressure value in 5800 RPM is already analyzed as represented in “Fig. 4” and the result is utilized in “Fig. 5”.

The inertia torque plot seems harmonic but in the case of gas pressure, the red dashed line reaches the maximum as well as minimum values. The torque value is negative when the gas pressure is applied, but it turns to maximum value after the combustion step. The total gas

pressure torque is calculated with resultant of the four torque plots for four pistons.

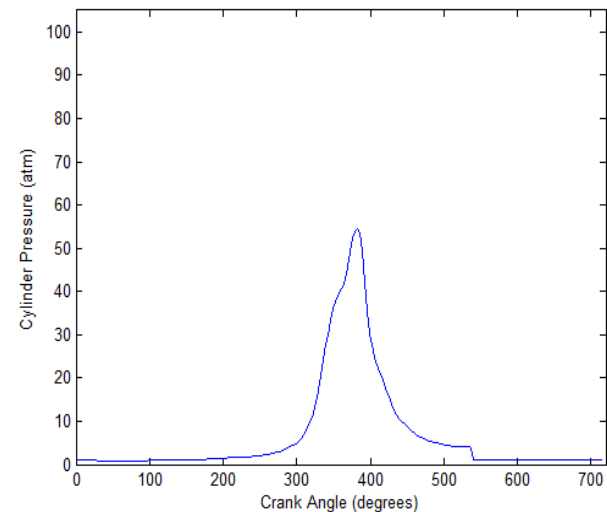


Fig. 4 Gas pressure on the piston at 720 degrees of engine rotations with 100 HP.

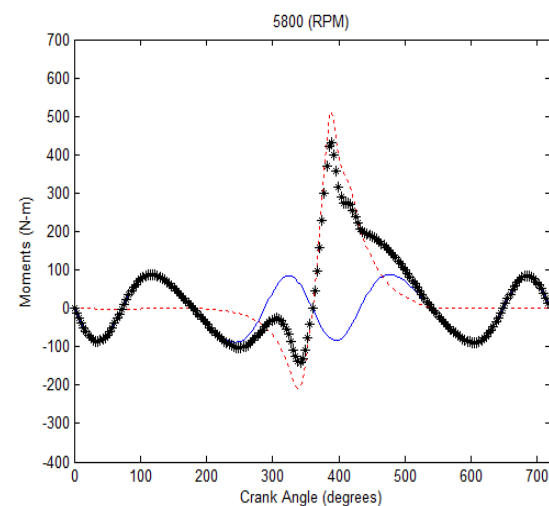


Fig. 5 Inertia torque (blue line) and gas pressure torque (red dashed line) and resultant torque on a piston (black starred line) in rotation velocity of 5800 RPM.

The friction torque (M_f) includes friction of piston with involved parts such as box and ring, and friction of box with involved elements such as camshaft, bearing under loading, or without loading. Thus the total friction torque value for different piston engines is obtained as below regarding [29]. The total friction torque value is approximately 4% lower of the sum of inertia and gas pressure torque and, thus the torque resulted from friction forces is neglected.

$$\sum M_f < 0.04 \times (M_g + M_i) \quad (13)$$

Besides, the value of M_I is approximately negligible due to the lack of any considerable applied load on the system. The gravity torque (M_G) is also negligible due to flat engine type that its equivalent torque is approximately zero. Consequently, the total torque of the system is obtained. By the way, “Eq. (14)” is for calculation of variations of angular acceleration.

$$\sum M = \sum I \ddot{\theta} \tag{14}$$

Figure 6 shows the gas pressure resultant torque plot in the 720-degree of engine rotation for four pistons without considering the phase difference due to different rotating velocities. Finally, the total torque plot is obtained in 5800 RPM.

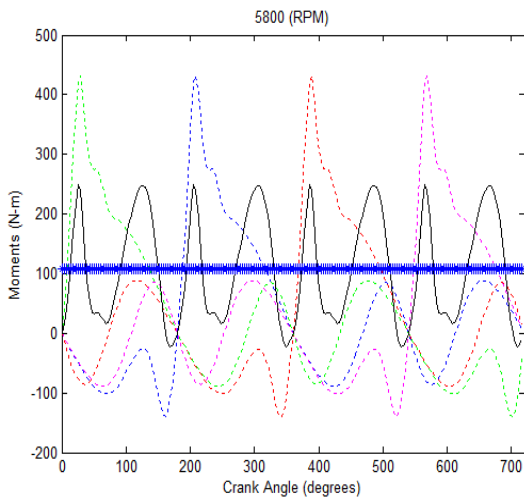


Fig. 6 Gas pressure torque (red, blue, green, purple dashed lines for four pistons), the resultant of gas pressure torque (black line) and the total torque (blue line) for 100 HP engine, 5800 RPM.

The obtained total torque value is shown in “Table 2” and compared with experiment. The difference in results is lower than 2% that has acceptable accuracy.

Table 2 Comparison of calculated and experimental torque in 5800 RPM velocity

Result	Experimental	Theoretical	Difference
Torque (N.m)	106.1	108	1.84%

5 NATURAL FREQUENCY

In the case of angular acceleration calculation, the difference value of the average of torques from the total torque is calculated then the remained plot is divided by the value of inertia torque as based on “Eq. (14)”. Figure

7 shows the variations of angular acceleration in a complete engine rotation of 5800 RPM.

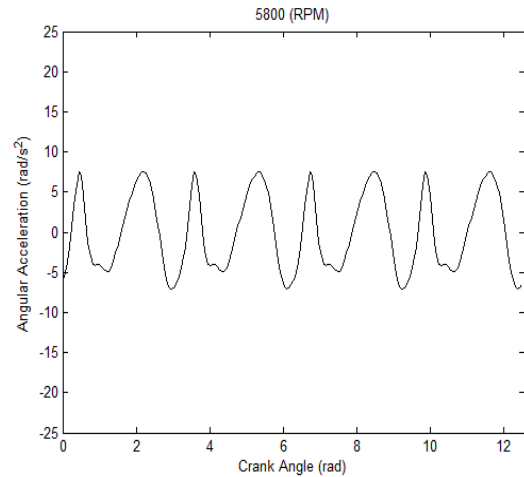


Fig. 7 Angular acceleration variations plot in a complete engine rotation cycles (4π), 5800 RPM.

The integration of the angular acceleration variations term concludes variation of angular velocity using MATLAB software and repeating the mathematical action leads to variations of angular displacement as shown in “Fig. 8”.

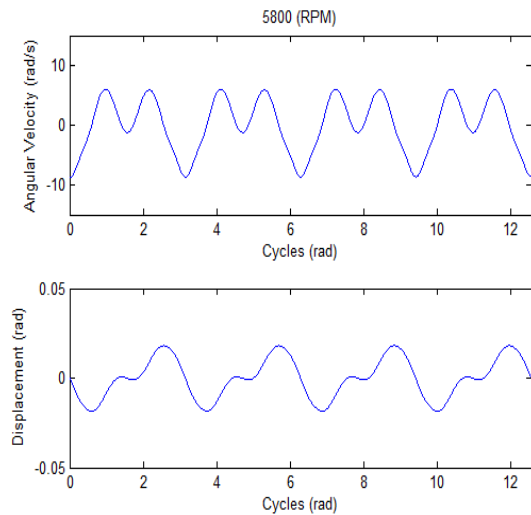


Fig. 8 Variation of angular velocity and displacement in rotating velocity of 5800 RPM.

The variation of angular velocity ratio versus different rotating velocity is represented in “Fig. 9”, which shows a slight decrease of angular velocity variations ratio as $\frac{\Delta\dot{\theta}}{\theta} = 0.026$ to $\frac{\Delta\dot{\theta}}{\theta} = 0.0241$ with increasing engine angular velocity in the range of 3800 to 5800 RPM, that are approximately equal. In other words, the phase

difference of different angular velocities during engine rotations is not considered in our calculations.

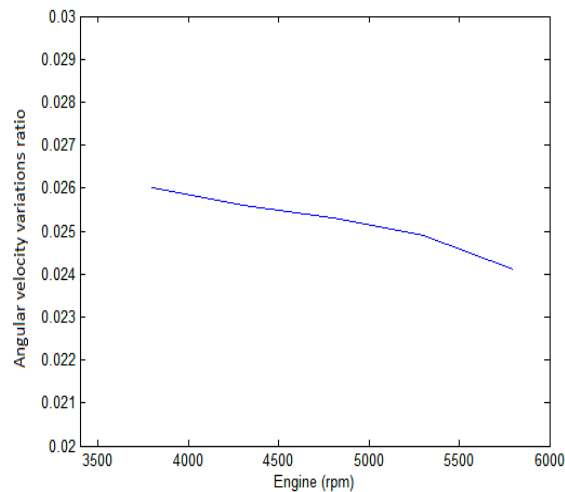


Fig. 9 variations of angular velocity ratio versus different angular velocity.

In order to select the suitable vibration damper, natural frequencies of the system are required. Due to the limitations of theoretical analysis, hardware requirements and economic problems, it is not possible to use the experimental testing process to obtain natural frequency, so numerical simulation is used. According to “Fig. 8”, variations of angular displacement was calculated using MATLAB software. In order to validate the modeling results, numerical analysis is employed, thus the crankshaft, pistons, propeller, and other sidepieces arrays are modeled and assembled using SolidWorks software as shown in “Fig. 10”. Each part is separately modeled and assembled for complete structure design using the assembly option of the software. The designed model was entered into Adams software environment to investigate angular displacement and natural frequency of system.

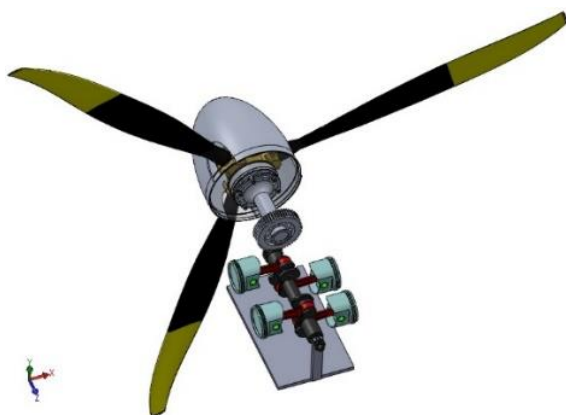


Fig. 10 Modeling of assembly of the piston, connecting rod, crankshaft and propeller arrays using SolidWorks software.

In the next step, the model is transferred to Adams software environment in STEP format with the module of (Adams/ Engine). The pendulum test which is one of the common methods to obtain inertia torque of an object with irregular geometry, is used to obtain the inertia torque of the connecting rod. The vibrations period of the connecting rod of 0.615 sec is obtained from the test that is repeated for all parts of system. The variation of angular velocity that is resulted from the test in engine rotation of 5800 RPM is described in “Fig. 11” in the case of the connecting rod. The Fast Fourier Transform (FFT) analysis is represented in “Fig. 12”.

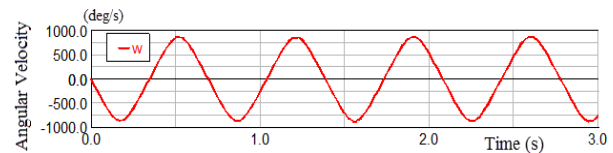


Fig. 11 Angular velocity versus time of the connecting rod from pendulum test from Adams software.

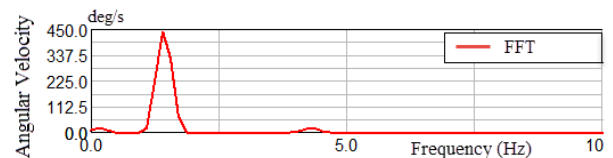


Fig. 12 FFT curve of connecting rod in Adams Software.

The maximum angular displacement variation has a peak to peak distance of 0.0365 Rad calculated from MATLAB software, and has a value of 0.0358 Rad obtained from Adams software. “Table 3” describes the difference between theoretical and modeled results that confirms accuracy of results, so the natural frequency of system can be achieved. The Frequency modes of system are obtained in “Table 4”.

Table 3 Peak to peak maximum displacement in 5800 RPM velocity

Result	Theoretical	Modeled	Difference
Displacement (Rad)	0.0365	0.0358	1.91%

Table 4 Modes of vibrations from Adams software

Frequency	Mode 1	Mode 2	Mode 3
Torsional Natural frequency (Hz)	381.34	521.18	956.76

6 DETERMINATION OF DYNAMIC ABSORBER

According to Equations (1-11), the dynamic absorber properties are determined, the damping coefficients are shown in “Fig. 13”, which describes the relation between transmission coefficient (X_1/X_2) and frequency ratio

(ω/ω_n) for different damping ratios. The damping ratio is selected between 0.05 to 1 if the amount of (ω/ω_n) is more than $\sqrt{2}$, while the value of 1 to 5 is related to (ω/ω_n) lower than 1. The variations of engine torque and maximum angular displacement are 286 N.m. and 0.0365 Rad respectively. Thus, the minimum damping capability of dynamic absorber is obtained 14.21 (N.m/Rad). Considering the natural frequency of 380 Hz, the damping ratio is selected in the range of 1 to 5.

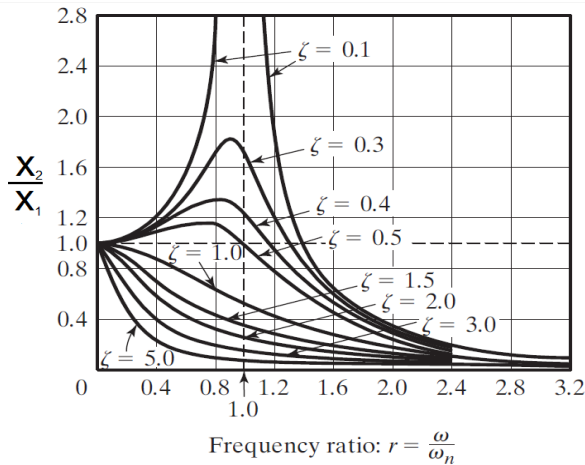


Fig. 13 Variations of transmission coefficient versus frequency ratio [11].

To compare the damping capability of dynamic absorber with different masses, two dynamic absorber of 50 and 100 g were investigated. Figures 14-15 show changes in the damping coefficient of 100 and 50 g of dynamic absorber, respectively. Doubling the absorber mass does not significantly increase the damping coefficient, and due to the mass limitations of using eight dynamic absorber connected in pairs in a four-piston engine, the 50g absorber is selected.

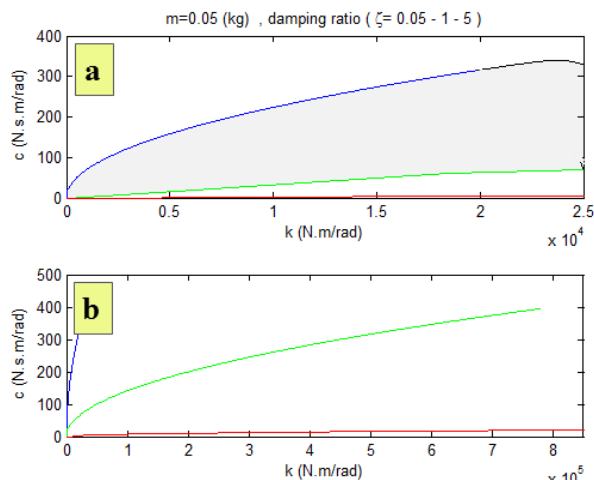


Fig. 14 a) Damping coefficient variation versus stiffness of a 100-gram absorber, b) magnification part of a).

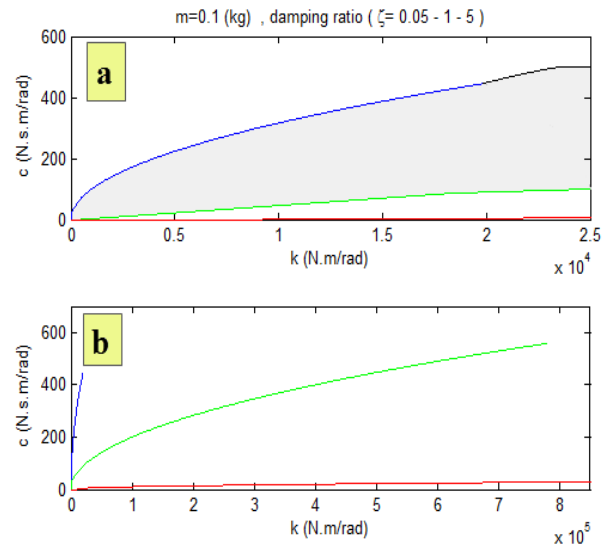


Fig. 15 a) Damping coefficient versus stiffness of a 50-gram absorber, b) magnification part of a).

Figure 16 represents the maximum angular displacement with (blue line) and without (red line) dynamic absorber which at least 40% of vibrations amplitude is decreased by using an absorber. Peak to peak distance of curves with and without absorber are 0.022 and 0.0365 Rad, respectively. When the value of displacement is close to zero, the displacement values are approximately equal with and without dynamic absorber, but the differences of values turn to increase with increasing displacement. In other words, damping capability will increase with increasing displacement as well as vibrations.

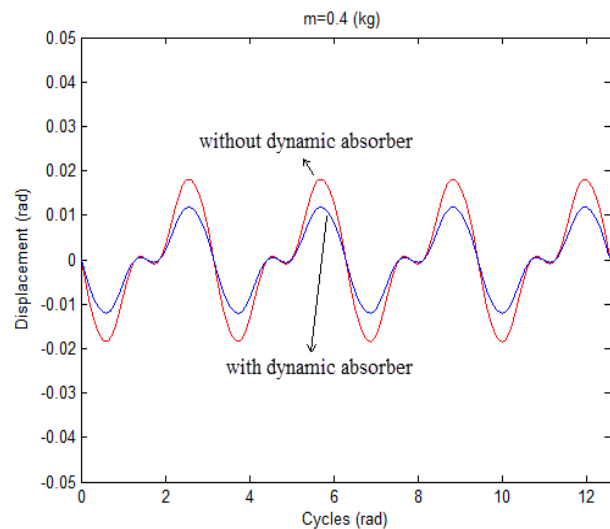


Fig. 16 Maximum displacement curves with and without dynamic absorber as blue and red lines, respectively.

It might seem that using a flywheel decreases the engine vibrations instead of dynamic absorber but it increases the weight of the system and also the system balance

turns into a practical difficulty. Thus the best way for decreasing the vibrations is by using a dynamic absorber.

7 CONCLUSION

The main purpose of this research was vibrations reduction of the ultralight aircraft engine to provide body safety in working condition of engine in flight. In the first step, the analytical equations of the dynamic absorber were calculated. Afterward, experimental measurement of gas pressure torque and total torque was carried out in the rotating velocity range of 1849 to 5800 RPM. Due to the limitations of experimental testing, theoretical analysis of system was calculated and implemented as code in MATLAB software. In order to verify the written code, the torques applied to the system and the amount of pressure applied to the piston were compared with the experimental results, which showed a difference of less than 2%. Beside, variations of angular velocity ratio in different rotating velocities represent a constant ratio approximately that is attributed to all engine rotation range, leading to approximately similar variations of displacement and vibrations.

For vibration analysis of the system, according to the limitations of theoretical analysis, the exact specifications of various components of the ultralight aircraft engine were assembled by reverse engineering, especially the propeller was modeled by 3D scanning and converting cloud points to solid model in SolidWorks software. Adams software was used to analyze natural frequencies of the system. The variations of angular displacement obtained from numerical and theoretical methods has a difference of 1.91%, which confirmed the simulation results.

In order to reduce the engine vibrations, using the dynamic absorber characteristics obtained from the analytical equations and considering the mass limitations, the damping coefficient of two dynamic absorbers of 50 and 100 g was compared. Due to the lack of significant increase in damping capability by doubling mass, the 50 g absorber was used. The results showed that the use of eight 50 g dampers, which are connected in pairs, can reduce the vibration amplitude of the system up to 40%.

8 NOMENCLATURE

C_t	Damping coefficient of the absorber (N.m.s/rad)
I	Inertia torque(kg.m ²)
K_0	Transformation ratio

K_t	Torsional stiffness (N.m/rad)
m	Absorber mass
x	Position of piston
\dot{x}	Velocity of piston
\ddot{x}	Acceleration of piston
M	Torque (N.m)
r	Radius of crankshaft

Greek symbols

θ_1	Vibration amplitude without dynamic absorber
θ_2	Vibration amplitude with dynamic absorber
$\dot{\theta}$	Angular velocity (rad/s)
$\ddot{\theta}$	Angular acceleration (rad/s ²)
ω	Frequency (rad/s)
ω_n	Natural frequency

REFERENCES

- [1] Feyzi, T., Tikani, R., Esfahanian, M., and Ziaei Rad, S., Performance Analysis of Different Modified Mr Engines Mounts, Journal of Solid Mechanics, 2011.
- [2] Taylor, C. F., Aircraft Propulsion, Smithsonian Annals of Flight, Vol. 1, No. 4, 1971.
- [3] Lee, E. C., Nian, C. Y., and Tarn, Y. S., Design of a Dynamic Vibration Absorber Against Vibrations in Turning Operations, Journal of Materials Processing Technology, Vol. 108, No. 3, 2001, pp. 278–285.
- [4] Higashi, K., Okamoto, S., Nagano, H., Yamada, Y., Effects of Mechanical Parameters on Hardness Experienced by Damped Natural Vibration Stimulation, 2015.
- [5] Mousavi, S. A., Rahmani, M., Kaffash Mirzarahimi, M., and Mahjoub Moghadas, S., The Dynamic and Vibration Response of Composite Cylindrical Shell Under Thermal Shock and Mild Heat Field, Journal of Solid Mechanics, Vol. 12, No. 1, 2020, pp. 175–188.
- [6] Ryabov, I. M., Chernyshov, K. V., Pozdeev, Comparative Evaluation of the Vibration Isolation Properties of a Suspension with Different Flywheel Dynamical Absorbers of the Car Body Oscillations, Procedia Engineering, Vol. 129, 2015, pp. 480–487.
- [7] Simakov, O. B., Mikhalkin, I. K., and Ponomarev, Y. K., Experimental Research of Ultra Small Vibration Dampers for Protection Against Vibration of Memory Units in Automatic on-board Systems on Vehicles, Procedia Engineering, Vol. 176, 2017, pp. 429–437.
- [8] Genta, G., On the Stability of Rotating Blade Arrays, Journal of Sound and Vibration, Vol. 273, No. 4–5, 2004, pp. 805–836.

- [9] Genta, G., Feng, C., and Tonoli, A., Dynamics Behavior of Rotating Bladed Discs: A Finite Element Formulation For The Study of Second And Higher Order Harmonics, *Journal of Sound and Vibration*, Vol. 329, No. 25, 2010, pp. 5289–5306.
- [10] Lin, S. M., Lee, S. Y., and Wang, W. R., Dynamic Analysis of Rotating Damped Beams with an Elastically Restrained Root, *International Journal of Mechanical Sciences*, Vol. 46, No. 5, 2004, pp. 673–693.
- [11] Rao, S. S., Yap, F. F., *Mechanical Vibrations*. Singapore: Pearson Education Inc, 2010.
- [12] Turhan, Ö., Bulut, G., Linearly Coupled Shaft-Torsional and Blade-Bending Vibrations in Multi-Stage Rotor-Blade Systems, *Journal of Sound and Vibration*. Vol. 296, No. 1–2, 2006, pp. 292–318.
- [13] Yang, C. H., Huang, S. C., The Influence of Disk's Flexibility on Coupling Vibration of Shaft-Disk-Blades Systems, *Journal of Sound and Vibration*, Vol. 301, No. 1–2, 2007, pp. 1–17.
- [14] Mohtasebi, S. S., Afshari, H., and Mobli, H., Analysis of Crankshafts Vibrations to Compare the Dynamic Behavior, *Journal of Applied Sciences*, Vol. 6, No. 3, 2006, pp. 591–594.
- [15] Hu, X., Sun, Q., Li, G., and Bai, S., Numerical Investigation of Thermo-Hydraulic Performance of an Opposed Piston Opposed Cylinder Engine Water Jacket with Helical Fins, *Applied Thermal Engineering*, 2019.
- [16] Gao, J., Tian, G., Jenner, P., and Burgess, M., Intake Characteristics and Pumping Loss in The Intake Stroke of a Novel Small Scale Opposed Rotary Piston Engine, *Journal of Cleaner Production*, 2020.
- [17] Lu, X., Zhang, F., Liu, Y., and Wang, S., Analysis on Influences of Scavenging Ports Width to Scavenging Process Based on Opposed Piston Two Stroke Diesel Engine, In: *Energy Procedia*, 2019.
- [18] Liu, Y., Zhang, F., Zhao, Z., Cui, T., Zuo, Z., and Zhang, S., The Effects of Pressure Difference on Opposed Piston Two Stroke Diesel Engine Scavenging Process, In: *Energy Procedia*, 2017.
- [19] Grabowski, Pietrykowski, K., and Karpiński, P., The Zero-Dimensional Model of the Scavenging Process in the Opposed-Piston Two-Stroke Aircraft Diesel Engine, *Propulsion and Power Research*, 2019.
- [20] Hua, Y., Wong, W., and Cheng, L., Optimal Design of a Beam-Based Dynamic Vibration Absorber Using Fixed-Points Theory, *Journal of Sound and Vibration*, Vol. 421, 2018, pp. 111–131.
- [21] Fischer, O., Wind-Excited Vibrations—Solution by Passive Dynamic Vibration Absorbers of Different Types, *Journal of Wind Engineering and Industrial Aerodynamics*, Vol. 95, No. 9–11, 2007, pp. 1028–1039.
- [22] Taghipour, J., Dardel, M., and Pashaei, M. H., Vibration Mitigation of a Nonlinear Rotor System with Linear and Nonlinear Vibration Absorbers, *Mechanism and Machine Theory*, Vol. 128, 2018, pp. 586–615.
- [23] Hafezalkotob, A., Hafezalkotob, A., Risk-Based Material Selection Process Supported on Information Theory: a Case Study on Industrial Gas Turbine, *Applied Soft Computing*, Vol. 52, 2017, pp. 1116–1129.
- [24] Lee, C. Y., Lin, J. H., Incorporating Piezoelectric Energy Harvester in Tunable Vibration Absorber for Application in Multi-Modal Vibration Reduction of a Platform Structure, *Journal of Sound and Vibration*. Vol. 389, 2017, pp. 73–88.
- [25] Ibrahim, R. A., Recent Advances in Nonlinear Passive Vibration Isolators, *Journal of Sound and Vibration*, Vol. 314, No. 3–5, 2008, pp. 371–452.
- [26] Hemati, Tajdari, and Khoogar, Roll Vibration Control for a Full vehicle Model Using Vibration Absorber, *International Journal of Automotive Engineering*, Vol. 3, No. 4, 2013.
- [27] Marzbanrad, J., Jamali, and Shakhilavi, S., A Biomechanical Modeling of an Automotive Passenger Body to Investigate the Vertical Vibration in Various Road Profiles Using Transmissibility Analysis, *International Journal of Automotive Engineering*, Vol. 7, No. 1, 2017.
- [28] Mahjoub-Moghadas, S., Internal Combustion Engines Control And Diagnostics Through Instantaneous Speed Of Rotation Analysis, Thesis Of PHD, L'ensam-Paris, 1985.
- [29] Najafzadeh, M., Fault Control and Detection in Internal Combustion Engines Through Angular Velocity and Vibration Analysis, 2007.